Vibrational Analysis and Spectra of Orotic Acid

ANTONIO HERNANZ,[1] FERENC BILLES,[2] IOAN BRATU,[3] RAQUEL NAVARRO[1]

[1] Departamento de Ciencias y Técnicas Fisicoquímicas, Universidad Nacional de Educación a Distancia, Senda del Rey s/n, E-28040 Madrid, Spain

[2] Department of Physical Chemistry, Technical University of Budapest, H-1521 Budapest XI, Budafoki ut 8, Hungary

[3] Institute of Isotopic and Molecular Technology, P.O. Box 700, R-3400, Cluj-Napoca 5, Romania

Received 29 April 1999; revised 3 June 1999; accepted 9 December 1999

ABSTRACT: The IR and Raman spectra of polycrystalline anhydrous orotic acid and its N1, N3, and O12 trideuterated isotopomer are recorded in the 4000–40 cm^{-1} spectral interval as part of a series of vibrational analyses of nucleosides, nucleotides, and related compounds carried out in our laboratory. The frequencies of the fundamental transitions and the potential energy distributions of the 39 normal modes of orotic acid and its isotopomer are calculated by an *ab initio* density functional theory Becke3P86/6-311G** treatment. Assignments of the vibrational modes are proposed that consider the results of these calculations and the observed spectra. The results of the *ab initio* treatment are related to crystallographic and spectral data, and they are compared with previous assignments for similar molecules. © 2000 John Wiley & Sons, Inc. Biopolymers (Biospectroscopy) 57: 187–198, 2000

Keywords: orotic acid; 6-uracilcarboxylic acid; vitamin B_{13}; density functional theory; IR; Raman

INTRODUCTION

In order to assign the vibrational spectra of nucleic acid components, a series of normal coordinate analyses of nucleosides, nucleotides, and related compounds was initiated in our laboratory.[1–6] Orotic acid (vitamin B_{13}, Fig. 1) and its salts play an important role in biological systems as precursors of pyrimidine nucleosides[7] and are found in cells and body fluids of many living organisms.[8–10] These compounds are applied in medicine as biostimulators of the ionic exchange processes in organisms, and different metal complexes of orotic acid were studied.[11–15] There is also a great interest in orotic acid in relation to food protection and nourishment research.[16–18] The crystal and molecular structure of orotic acid was determined by Takusawaga and Shimada,[19] and Mutikainen[20] studied the crystal structure of metal complexes of orotic acid.

Because of the importance of orotic acid and its metal complexes in living systems, a reliable assignment of their vibrational spectra is a useful basis in the study of their interactions with other chemical species present in the biological milieu. The orotic acid molecule is related to the molecules of uracil or thymine. Different studies on these type of molecules were done by vibrational spectroscopy,[21,22] as well as normal coordinate analysis (NCA) and *ab initio* calculations.[22–33] The results of these studies may help in the assignment of the spectra of orotic acid.

In this study the IR and Raman spectra of orotic acid were recorded in the 4000–40 cm^{-1} spectral interval. An optimized molecular struc-

Correspondence to: A. Hernanz (ahernanz@sr.uned.es).

Contract grant sponsor: Hungarian National Scientific Research Funds (OTKA); contract grant number: T 14064.

Biopolymers (Biospectroscopy), Vol. 57, 187–198 (2000)

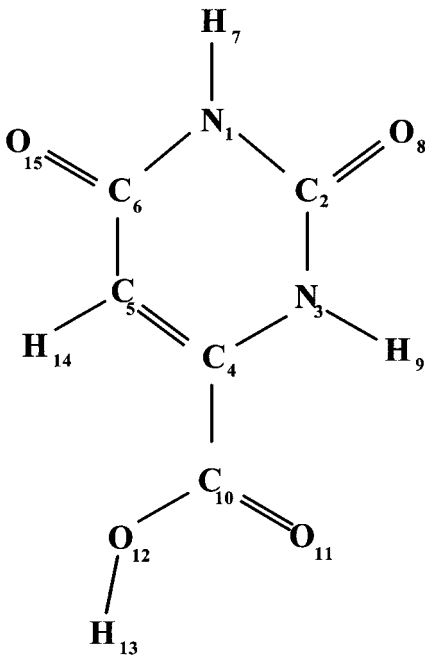

Figure 1. The atomic numbering system of orotic acid.

ture was obtained by applying an *ab initio* density functional theory (DFT) Becke3P86/6-311G** treatment. The *ab initio* optimized structure was compared with the structure of the molecule in the crystalline state obtained from X-ray diffraction. From the *ab initio* calculation an NCA was carried out with scaling to the experimental spectra. The frequencies of the fundamental transitions and the potential energy distributions (PEDs) of the 39 vibrational modes of orotic acid were calculated in this way. In order to get additional information for the assignment of the vibrational spectra of orotic acid, its N1, N3, and O12 trideuterated derivative (N1,N3,O12-^{2}H) was synthesized, the corresponding spectra were recorded, and an NCA with the scaled force field for the parent molecule was done. An assignment of the vibrational modes is proposed that considers the results of these calculations and the observed spectra. The assignment proposed is discussed considering previous assignments for similar molecules.

MATERIALS AND METHODS

Anhydrous orotic acid was purchased from Sigma Chemical Co. The IR spectra of polycrystalline orotic acid and its N1,N3,O12-^{2}H isotopomer were recorded with a Bomem DA3 spectrophotometer working under a vacuum (pressure $\leq$ 133.3 Pa) to eliminate IR absorption from atmospheric water and CO_2. The mid-IR region (Figs. 2, 3) was recorded using a Globar source, a DTGS detector, and a KBr beam splitter at an effective apodized resolution of s = 0.89 cm^{-1} (RES = 1 and Hamming apodizing function), coadding 500 interferograms to obtain a good signal to noise ratio. The far-IR (FIR) regions from 700 to 200 and 200 to 40 cm^{-1} (Fig. 4) were recorded coadding 1000 interferograms and using s = 1.77 cm^{-1} (RES = 2 and Hamming apodizing function) with a DTGS-FIR detector and a high pressure mercury lamp. Mylar beam splitters of 3 and 12 μm were used for the former and the latter FIR regions, respectively.

The FT-Raman spectra shown in Figures 5 and 6 were recorded with a Bomem DA3/DA8 FT-Raman accessory. The exciting source was a xenon lamp pumped Nd^{3+}-YAG laser working at 1064 nm with powers of 300 and 700 mW at the sample position for orotic acid and its isotopomer, respectively. A quartz beam splitter and an indium gallium arsenide (InGaAs) detector working

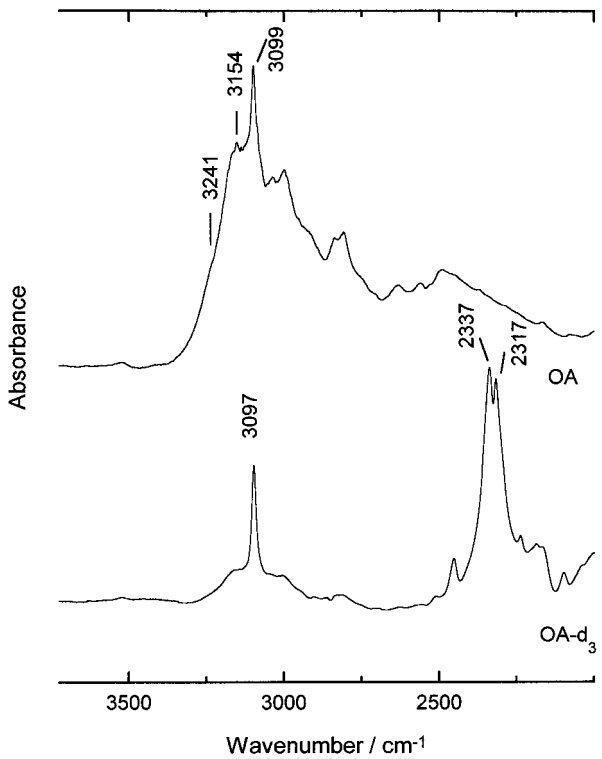

Figure 2. IR spectra (3000 cm^{-1} region) of polycrystalline orotic acid (OA) and its N1,N3,O12-^{2}H isotopomer (OA-d_3) in KBr.

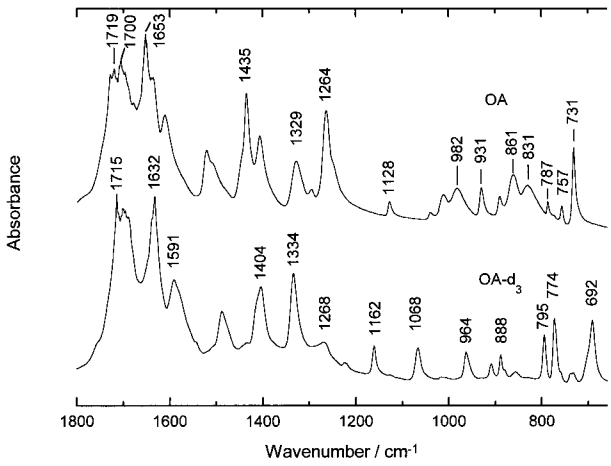

Figure 3. IR spectra (1800–660 cm^{-1} region) of polycrystalline orotic acid (OA) and its N1,N3,O12-^{2}H isotopomer (OA-d_3) in KBr.

at 300 K were used. The resolution was s = 4.0 cm^{-1} (Blackman–Harris apodizing function) and 1000 interferograms were coadded. Wavenumber shift calibration with acetamidophenol[34] in the range of 3326.6–213.3 cm^{-1} using the same recording conditions gave a mean deviation of 0.5 cm^{-1}.

Synthesis of N1,N3,O12-^{2}H Isotopomer

The N—H and O—H bonds are strongly polarized; consequently, the hydrogen atoms of these groups have an acid character allowing a self-catalyzed isotopic exchange reaction through the

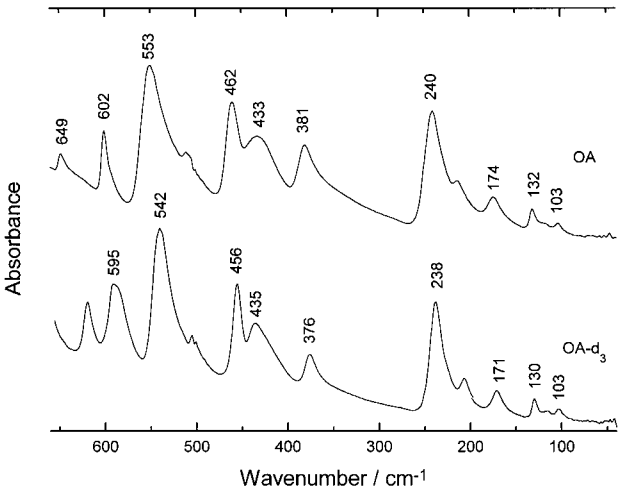

Figure 4. Far-IR spectra (660–40 cm^{-1} region) of polycrystalline orotic acid (OA) and its N1,N3,O12-^{2}H isotopomer (OA-d_3) in a polyethylene disk.

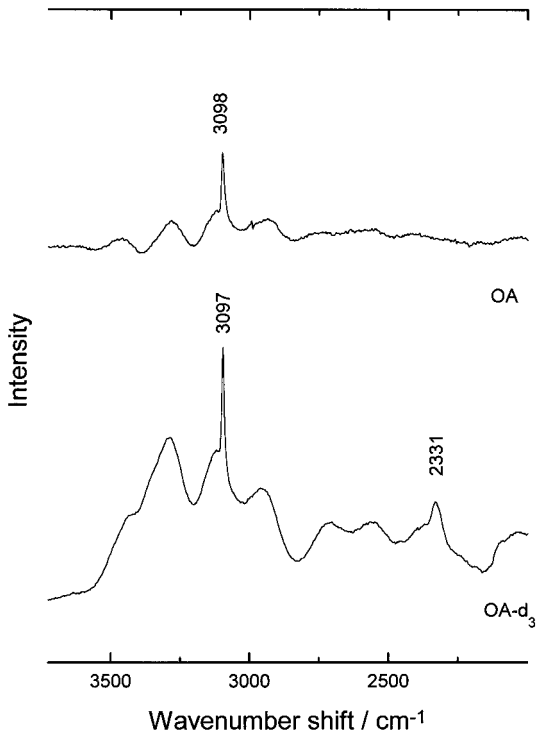

Figure 5. FT-Raman spectra (3000 cm^{-1} region) of polycrystalline orotic acid (OA) and its N1,N3,O12-^{2}H isotopomer (OA-d_3).

protons emitted by orotic acid in aqueous solution. Because of the low solubility of the acid in water, an emulsion was prepared of orotic acid in deuterium oxide with a ratio of 4/100 in organic hydrogen atoms/deuterium aqueous atoms. It was

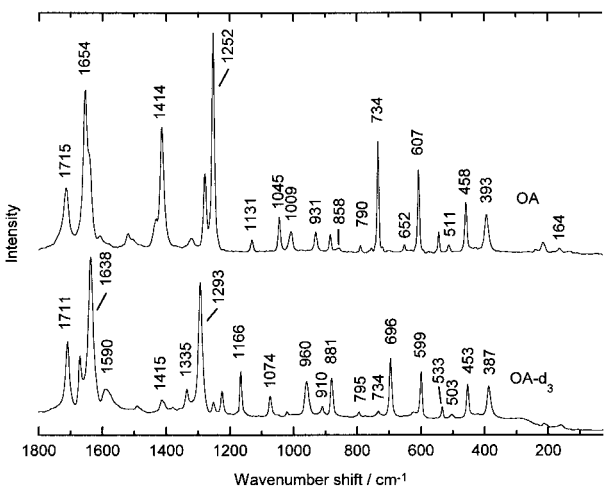

Figure 6. FT-Raman spectra (1800–40 cm^{-1} region) of polycrystalline orotic acid (OA) and its N1,N3,O12-^{2}H isotopomer (OA-d_3).

Table I. Definition of Internal Coordinates for Orotic Acid

1 $r_{1,2}$	21 $\varphi_{6,1,2} - \varphi_{5,6,1} + \varphi_{3,4,5} - \varphi_{2,3,4}$
2 $r_{2,3}$	22 $\vartheta_{7,2,1,6}$
3 $r_{3,4}$	23 $\vartheta_{8,3,2,1}$
4 $r_{4,5}$	24 $\vartheta_{9,2,3,4}$
5 $r_{5,6}$	25 $\vartheta_{10,3,4,5}$
6 $r_{6,1}$	26 $\vartheta_{14,4,5,6}$
7 $r_{1,7}$	27 $\vartheta_{15,1,6,5}$
8 $r_{2,8}$	28 $\tau_{6,1,2,3} - \tau_{1,2,3,4} + \tau_{2,3,4,5} - \tau_{3,4,5,6} + \tau_{4,5,6,1} - \tau_{5,6,1,2}$
9 $r_{3,9}$	29 $\tau_{1,2,3,4} - \tau_{3,4,5,6} + \tau_{4,5,6,1} - \tau_{6,1,2,3}$
10 $r_{4,10}$	30 $\tau_{6,1,2,3} - 2\tau_{1,2,3,4} + \tau_{2,3,4,5} + \tau_{3,4,5,6} - 2\tau_{4,5,6,1} + \tau_{5,6,1,2}$
11 $r_{5,14}$	31 $r_{10,11}$
12 $r_{6,15}$	32 $r_{10,12}$
13 $\varphi_{6,1,7} - \varphi_{2,1,7}$	33 $r_{12,13}$
14 $\varphi_{1,2,8} - \varphi_{3,2,8}$	34 $\varphi_{4,10,11}$
15 $\varphi_{4,3,9} - \varphi_{2,3,9}$	35 $\varphi_{4,10,12}$
16 $\varphi_{3,4,10} - \varphi_{5,4,10}$	36 $\varphi_{10,12,13}$
17 $\varphi_{6,5,14} - \varphi_{4,5,14}$	37 $\tau_{12,10,4,5}$
18 $\varphi_{1,6,15} - \varphi_{5,6,15}$	38 $\tau_{11,10,4,3}$
19 $\varphi_{1,2,3} - \varphi_{6,1,2} + \varphi_{5,6,1} - \varphi_{4,5,6} + \varphi_{3,4,5} - \varphi_{2,3,4}$	39 $\tau_{13,12,10,4}$
20 $2\varphi_{1,2,3} - \varphi_{6,1,2} - \varphi_{5,6,1} + 2\varphi_{4,5,6} - \varphi_{3,4,5} - \varphi_{2,3,4}$	

r, stretching; φ, in-plane bending; ϑ, out of plane bending; τ, torsion.

stirred for several hours at room temperature. The orotic acid was separated, deuterium oxide was added to this fraction, and it was stirred again. This process was repeated until equilibrium was observed in the IR spectra of the remaining fraction with deuterium oxide.

Ab Initio Calculations

The *ab initio* calculations were done using the Gaussian 92/DFT program.[35] The self-consistent field (SCF) treatment was applied for geometry optimization with the Direct and NOPAS options. Because of the size and type of the molecule, a method was adopted that takes electronic correlation into account: the hybrid method Becke3P86 for the DFT exchange functional. This could be considered an effective computational alternative to the second-order Møller–Plesset (MP2) method, provided that a reasonably sized basis is selected. From the point of view of vibrational spectroscopy, the 6-311G** basis set seems more appropriated than the 6-31G* because it is larger, more flexible, and the diffuse *p* function on the hydrogen atoms tends to compensate the anharmonic effects of the CH and NH stretches. For these reasons the hybrid functional DFT method Becke3P86 was used with a 6-311G** basis set. A workspace of 6 Mb was allowed. The vibrational force field and frequency calculations were carried out with the same functional and basis set. The quantum chemical results, optimized geometry, and the force constants matrix **F** (in Cartesian coordinate representation) were used for an NCA. The Wilson method was applied for this purpose using a program developed by Billes.[36] The kinetic energy matrix, **G**, was built up from a set of independent internal coordinates (Table I) and the optimized molecular geometry. The **F** matrix was transformed into internal coordinate representation and the corresponding **GF** matrix eigenvalues were calculated. The **F** matrix was scaled to the experimental frequencies by applying scale factors. These factors were optimized using the method of weighted least squares. A new **GF** eigenvalues calculation was carried out with these scale factors. The result gave the scaled **F** matrix, the calculated frequencies, and the PED matrix.

RESULTS AND DISCUSSION

The optimized molecular structure turned out to be very close to the structure obtained by X-ray diffraction (Table II).[19] The bond lengths were

Table II. Experimental (X-ray Diffraction[19]) and Calculated (DFT, Becke3P86/6-311G**) Geometrical Parameters of Orotic Acid

Parameter	X-ray	DFT	Parameter	X-ray	DFT
N1—C2	1.373	1.381	C6—N1—C2	126.4	128.5
C2—N3	1.363	1.386	N1—C2—N3	114.7	112.9
N3—C4	1.365	1.370	C2—N3—C4	122.7	123.5
C4—C5	1.346	1.347	N3—C4—C5	121.7	122.0
C5—C6	1.433	1.456	C4—C5—C6	119.0	119.8
C6—N1	1.369	1.402	C5—C6—N1	115.5	113.4
N1—H7	0.890	1.011	C6—N1—H7	117.0	116.2
C2—O8	1.227	1.207	N1—C2—O8	121.2	124.2
N3—H9	0.940	1.009	C4—N3—H9	121.0	120.1
C4—C10	1.498	1.491	N3—C4—C10	114.1	117.7
C10—O11	1.197	1.198	C4—C10—O11	120.5	124.6
C10—O12	1.306	1.345	C4—C10—O12	114.1	111.3
O12—H13	1.020	0.967	C10—O12—H13	105.0	107.3
C5—H14	1.030	1.079	C4—C5—H14	124.0	120.8
C6—O15	1.237	1.210	N1—C6—O15	119.5	121.0

Bond lengths are in angstroms and angles are in degrees.

similar. The higher differences of 0.121, 0.069, 0.053, 0.049, and 0.039 Å correspond to increases of the bond lengths N1—H7, N3—H9, O12—H13, C5—H14, and C10—O12, respectively,[19] as well as to the C2═O8 and C6═O15 bonds, which shorten 0.020 and 0.027 Å, respectively. The involvement of these groups in hydrogen bonds and other intermolecular interactions in the crystal would account for these differences. The angles were also similar and the higher differences were observed in the carboxylic group. This could be considered as additional effects of the intermolecular forces acting on the polar groups in the crystal. The molecule maintained a planar structure (Table III).

The wavenumber of the fundamental transitions and the PED for the vibrational modes calculated by the *ab initio* DFT Becke3P86/6-311G** treatment are given in Tables IV and V. The spectra of orotic acid and its N1,N3,O12-^{2}H deuterated derivative are shown in Figures 2–6. The resulting scale factors are given in Table VI. There are 11 different factor values; eight scale factor values are between 0.991 and 0.803. The three lower factor values of 0.729, 0.757, and 0.761 correspond to stretches of groups (νOH, νNH, and νC—Oca, respectively) presumably involved in intermolecular interactions, which was stated previously. The scaled wavenumbers of the fundamental transitions and the PED, as well as the observed wavenumbers, are listed in Tables VII and VIII. The mean deviations between calculated and observed wavenumbers for orotic acid and the isotopomer are 30 and 27 cm^{-1} (3.8 and 3.9%), respectively, the larger deviations being localized on the amino out of plane deformations (OPD), γN—H; the H bonds shift these vibrations to 890–810 cm^{-1}. The difficulties in reaching an accurate scaling of the γN—H motions in uracil were pointed out by Aamouche et al.[32] when the wavenumbers of this molecule were calculated at the SCF+MP2 level. Perturbations from hydro-

Table III. Cartesian Coordinates (Å) Corresponding to *ab initio* DFT Becke3P86/6-311G** Optimized Geometry for Orotic Acid

Atom	*x*	*y*	*z*
N1	−1.083993	−0.147908	0.000000
C2	−0.982977	−1.530702	0.000000
N3	0.325642	−1.973177	0.000000
C4	1.503553	−1.212461	0.000000
C5	1.263238	0.223755	0.000000
C6	0.000000	0.690189	0.000000
H7	−2.018488	0.233677	0.000000
O8	−1.944769	−2.259290	0.000000
H9	0.442997	−2.977746	0.000000
C10	2.589537	−1.746298	0.000000
O11	2.102818	0.902143	0.000000
O12	−0.258223	2.158455	0.000000
H13	−1.577409	2.422749	0.000000
H14	−1.678677	3.384432	0.000000
O15	0.595923	2.999048	0.000000

Table IV. *Ab Initio* DFT Becke3P86/6-311G** Vibrational Fundamentals Calculated for Orotic Acid

Calculated Wavenumbers (cm^{-1})	Potential Energy Distribution (%)
3796	100νOH
3637	99νN3H9
3614	99νN1H7
3266	99νCH
1858	77νC═Oca
1849	67νC2═O8
1807	77νC6═O15
1698	74νrg
1537	45νrg, 26βN3H9
1413	35βN1H7, 29νrg, 12βN3H9, (βNH in opposite phase)
1411	33βN1H7, 32νrg, 6βN3H9, (βNH in phase), (6βC2═O8, 6βC6═O15 in opposite phase)
1389	24βOH, 18νC—Oca, 14νCrg—Cca, 12νrg, 10βC═Oca
1311	32βCH, 22βN3H9, 22νrg
1224	66νrg, 16βCH
1182	51βOH, 23νC—Oca
1113	38νrg, 28βCH, 16νC—Oca
1028	51βrg, 20νrg
1011	61νrg, 13βrg, 11βN1H7
923	56νrg, 14νCrg—Cca, 11βrg
890	61γCH, 15γrg, 13γCrg—Cca
797	54γCrg—Cca, 17γC═Oca, 15γC6═O15
779	70γC2═O8, 15γN1H7, 7γC6═O15 (γCO in phase)
749	(42γC6═O15, 20γC2═O8 in opposite phase), 14γrg, (9γN3H9, 3γN1H7 in phase)
690	69γN1H7, 20γrg, 3γN3H9 (γNH in opposite phase)
688	31βC═Oca, 17νrg, 12νC—Oca, 12βrg
625	(28βC2═O8, 26βC6═O15 in phase), 17νC—Oca
624	37γN3H9, 32γOH, 10γN1H7 (γNH in phase)
589	50γN1H7, 38γOH
578	45βrg, 28νrg, 10βC═Oca
531	76βrg
463	30γrg, 22γOH, 18γC═Oca, 16γC—Oca
432	29βC—Oca, 21βC═Oca, 17νrg, (9βC6═O15, 8βC2═O8 in opposite phase)
407	33βrg, (22βC6═O15, 21βC2═O8 in phase)
341	27νrg, 22νCrg—Cca, (13βC6═O15, 11βC2═O8 in phase), 10βrg
182	80γrg, 11γC═Oca
178	65βCrg—Cca, 11βC—Oca
155	90γrg
121	59γrg, 22γCrg—Cca
63	100γOH

ν, stretching; β, in-plane deformation; γ, out of plane deformation; rg, ring; ca, carboxylic group; βrg, linear combinations (l.c.) 19, 20, and 21 (Table I); γrg, l.c. 28, 29, and 30 (Table I). Only the higher potential energy distribution values are mentioned.

gen bonding and packing effects in the solid phase are argued. Isotopic shifts can be evaluated by comparing Tables VII and VIII. Nevertheless, changes in the PED between orotic acid and its isotopomer make it difficult to establish a correspondence between their normal modes. The assignment of the observed wave numbers by spectral regions, considering the nature of the normal modes, is presented below. The assignment of many wavenumbers agrees with the previous results for the parent molecules uracil[22,27,31,37–39] and thymine.[22,27,31,33,37]

3500–2000 cm^{-1} Spectral Region

In this region the O—H, N—H, and C—H stretches give rise to intense IR bands (Fig. 2, Tables VII and VIII. The assignment of the O—H

Table V. *Ab Initio* DFT Becke3P86/6-311G** Vibrational Fundamentals Calculated for N1,N3,O12-^{2}H Deuterated Derivative of Orotic Acid

Calculated Wavenumbers (cm^{-1})	Potential Energy Distribution (%)
3266	99νCH
2762	99νOD
2668	98νN3D9
2649	98νN1D7
1852	85νC═Oca
1838	73νC2═O8, 7νC6═O15 (in phase)
1797	74νC6═O15, 6νC2═O8 (in phase)
1693	76νrg
1503	60νrg, 11βrg
1385	57νrg, (13βC2═O8, 9βC6═O15 in phase)
1311	34νC—Oca, 16βCH, 16βC═Oca, 14νCrg—Cca
1287	58νrg, 17βN1D7
1219	56νrg, 18βN3D9, 12βCH
1148	36βCH, 21νrg, 19βN1D7, (8βC2═O8, 6βC6═O15 in phase)
1045	34νC—Oca, 20βOD, (7βN3D9, 3βN1D7 in opposite phase)
996	58βrg, 16νrg, 13βOD
968	27βN3D9, 25βOD, 21νrg, 5βN1D7, (βND in opposite phase)
890	60γCH, 14γrg, 13γCrg—Cca, 10γC6═O15
886	54νrg, 10βrg, 9βN3D9
847	39νrg, (39βN1D7, 15βN3D9 in phase)
793	57γCrg—Cca, 16γC═Oca, 15γC6═O15
775	86γC2═O8, 8γC6═O15 (in phase)
740	52γC6═O15, 21γrg, 13γC2═O8, (γCO in opposite phase), 11γCH
634	21νrg, 19βC═Oca, 16βOD, 13βrg
595	(25βC2═O8, 18βC6═O15 in opposite phase), 11βC—Oca, 10βCrg—Cca
561	37βrg, 17βC═Oca, 17νrg, 11βC—Oca
560	26γN1D7, 24γrg, 19γC—Oca, 19γC═Oca, 10γCrg—Cca, 10γOD, 4γN3D9, (γND in phase)
517	70βrg, (9βC6═O15, 4βC2═O8 in opposite phase)
491	71γN1D7, 14γOD
447	85γN3D9, 12γrg
428	28βC—Oca, 20βC═Oca, 17νrg, (10βC6═O15, 8βC2═O8 in opposite phase)
400	30βrg, (25βC2═O8, 20βC6═O15 in phase), νrg10
389	71γOD, 18γrg
338	26νrg, 23βCrg—Cca, (13βC6═O15, 9βC2═O8 in phase), 12βrg, 11βC—Oca
180	80γrg, 10γC═Oca
174	65βCrg—Cca, 12βC—Oca
150	83γrg
118	58γrg, 24γCrg—Cca
62	55γC—Oca, 34γC═Oca, 11γrg

The code for the symbols is described in the footnote of Table IV. Only the higher potential energy distribution values are mentioned.

and N—H stretching bands is rather difficult. These bands appear overlapped in the same spectral region, and the involvement of these groups in hydrogen bonds[19] affects their wavenumbers and produces a relevant band broadening. X-ray diffraction data indicate that the two amino groups have similar hydrogen bond lengths.[19] This suggests that both groups are involved in hydrogen bonds of the same energy,[40] and therefore the position of the νN1H7 and νN3H9 stretching bands would depend more on intramolecular than on intermolecular effects. The N1H7 stretch appears at lower wave number values than the N3H9 stretch (Tables IV, V, VII, and VIII). This is consistent with the suggestion that the second proton ionization of orotic acid is from

Table VI. Factors for Scaling Vibrational Force Field of Orotic Acid with *Ab Initio* B3P86/6-311G** Treatment

Coordinates	Factor	Coordinates	Factor
νC═Crg	0.879	γCH	0.879
νCNrg	0.879	γCrg—Cca	0.803
νCCrg	0.879	γNH	0.879
νC═Org	0.864	γrg	0.803
νCH	0.900	νC—Oca	0.761
νCrg—Cca	0.879	νC═Oca	0.864
νNH	0.757	νOH	0.729
βC═Org	0.991	βC—Oca	0.991
βCH	0.803	βC═Oca	0.991
βrg—Cca	0.980	βOH	0.830
βNH	0.830	γC—Oca	0.990
βrg	0.980	γC═Oca	0.990
γC═Org	0.990	γOH	0.879

The code for the symbols is described in the footnote of Table IV.

the N1H7 group rather than the N3H9 group, and it contradicts the assumption of M'Boungou et al.[42] that was formulated in the opposite sense. The presence of the νN1H7 and νN3H9 bands in this region and the appearance of the νC2═O8 and νC6═O15 bands in the region of $\approx$1700 cm^{-1} are further evidence that confirms that the molecule is in the tautomeric keto form in the crystal.[19] The νO12H13, νN3H9, and νN1H7 bands undergo isotopic shifts to lower wavenumbers upon deuteration: $\Delta\nu$ = −881, −817, and −820 cm^{-1}, respectively (Tables VII and VIII, Figs. 3 and 5). The νC5H14 band overlaps with the N—H and O—H stretching bands, but it is much narrower as may be seen in Figures 3 and 5.

1800–900 cm^{-1} Spectral Region

The bands that appear in this region are mainly due to in-plane vibrations (Tables IV, V, VII, and VIII). Some mixed modes with ring and carboxylic contributions are observed in this region; a significant vibrational coupling between the ring and carboxylic moieties is predicted. The double bond stretching vibrations νC═O and νC═C are the internal coordinates that dominate in the modes with fundamentals in the 1800–1600 cm^{-1} spectral range. The results obtained for orotic acid and its isotopomer (Tables IV, V, VII, and VIII) indicate a considerable coupling among the carbonyl stretches. A complicated Fermi resonance effect was proposed for the two C═O stretching vibrations of uracil observed in the 1800–1700 cm^{-1} range.[43] The fundamental out of phase mixed carbonyl stretching vibration of uracil was unambiguously assigned[44] to the IR band at 1703.888 cm^{-1}. The nucleotide 5′-uracil monophosphate (5′-UMP) in H_2O solution shows the carbonyl stretching vibration of the uracil moiety[26] at 1681 cm^{-1}. The observation of νC═O bands active in the IR and Raman precludes the common arrangement of the molecules of carboxylic acids in centrosymmetric dimers[45] for the orotic acid. According to Takusawaga and Shimada[19] the molecules are arranged in parallel layers, each layer formed by chains of molecules. The significant contributions of the in-plane amino deformations βN1H7 and βN3H9 to the 1435, 1329, and 1264 (also βOH) cm^{-1} IR bands and to the 1414 and 1252 cm^{-1} Raman bands agree with the drastic effects observed upon deuteration (Figs. 3 and 6). Different stretches of the uracil ring contribute to the bands in the 1600–900 cm^{-1} region. The C4═C5 stretching vibration must be assigned to the strong Raman band at 1654 cm^{-1} (1653 cm^{-1} in IR). For uracil this vibration is assigned[43] to a strong Raman band at 1647 cm^{-1}. The assignment of all observed IR and Raman bands in this spectral range is difficult, because of the presence of highly coupled modes and combination bands that may overlap with those due to fundamentals, and they interact with one another, leading to distortions of the observed bands. Most of the isotopic shifts in this region cannot be established properly because of the lack of correspondence between the modes of the two isotopic species (i.e., their PEDs are not similar).

Below 900 cm^{-1} Spectral Region

In this spectral region the normal modes appear to be rather delocalized. Nevertheless, the IR bands at 831, 787, 649, 553, and 132 cm^{-1} are mainly due to vibrations of the uracil ring whereas the IR band at 174 cm^{-1} is mostly due to vibrations of the carboxylic group. The strong Raman band at 734 cm^{-1} is usually assigned in uracil and its derivatives to a ring breathing mode of the base. The nucleotide 5′-UMP in H_2O solution shows the uracil ring breathing vibration[26] at 785 cm^{-1}, and it is assigned by Tsuboi et al.[43] to one band in the 850–600 cm^{-1} range for crystalline uracil. Nevertheless, a dominant ring breathing mode has not been obtained for orotic acid. According to the results, this band would be assigned to the calculated wavenumber at 688

Table VII. Observed and Scaled Vibrational Fundamentals of Orotic Acid

Observed Wavenumbers		Calculated and Scaled Wavenumbers	
IR $\tilde{\nu}$ (cm^{-1})	Raman $\Delta\tilde{\nu}$ cm^{-1}	$\tilde{\nu}$ (cm^{-1})	Potential Energy Distribution (%)
3241 sh		3242	100νO12H13
3154mb		3166	99νN3H9
3137mb		3146	99νN1H7
3099 s	3098 w	3098	99νC5H14
1729 vs		1732	66νC═Oca, 17νC2═O8 (in phase)
1719 vs	1715 m	1725	56νC2═O8, 19νC═Oca (opposite phase)
1700 vs		1686	73νC6═O15, 11νrg
1653 vs	1654 s	1599	64νC4C5, 7νrg
1435 sb	1414 s	1439	35νN3C4, 18βN1H7, 14νrg, 11βrg
1329 m		1342	21νN1C2, 17βC2═O8, 16νrg, 13νN3C2, 12(βN1H7, βN3H9), 11βC6═O15 (βC═O in phase)
1313 ov		1299	63βN1H7, 16νrg, 15(νC2═O8, νC4═O10 opposite phase)
1264 sb		1283	26βOH, 17(βN1H7, βN3H9), 14νCrg—Cca, 15νC—Oca, 14βC═Oca
1248 sh	1252 s	1213	28νrg, 27βN3H9, 24βC5H14
1128 w	1131vw	1146	23νN1C6, 18βC5H14, 14νN1C2, 10νN3C2, 17(other νrg)
1041 w	1045 w	1078	49βOH, 12νCrg—Cca, 12νC—Oca
1012 w	1009 w	1022	40νrg, 28βC5H14, 12νC—Oca
982 m		986	56βrg, 20νC—Oca
931 m	931 w	948	22νN1C2, 29νN3C2, 16(βN1H7, βN3H9), 13(other νrg)
890 w	884 w	866	31νC5C6, 14νCrg—Cca, 12νN1C6, 10νC—Oca, 10νN3C2
861mb	858vw	642	63γN1H7, 30γrg
		846	61γC5H14, 20γC6═O15, 10γrg
831mb		588	33γN3H9, 32γOH, 14γN1H7, (γNH in phase)
787 w	790 w	780	64γC2═O8, 16(γN1H7, γN3H9), 12γrg, 6γC6═O15, (γC═O in phase)
757 w	753vw	754	33γCrg—Cca, (25γC6═O15, 16γC2═O8 opposite phase), 15γC—Oca
		715	27γC6═O15, 17γC5H14, 17γCrg—Cca, 10γC—Oca
731 m	734 s	656	28βC═Oca, 18νC—Oca, 14νrg, 14βC—Oca
649vw	652vw	554	52γN3H9, 33γOH
602 w	607 m	616	27βC2═O8, 25βC6═O15, 16βC—Oca, 13βCrg—Cca, (βC═O in opposite phase)
553 sb	543 w	559	45βrg, 30νrg
512vw	511vw	523	73βrg
462 m	458 m	438	32γrg, 28γOH, 14γC—Oca, 14γC═Oca
433wb		423	29βC—Oca, 20νrg, 20βC═Oca, 15(βC2═O8, βC6═O15 opposite phase)
381wb	393 w	399	30βrg, (22βC6═O15, 21βC2═O8 in phase), 11νrg
		328	29νrg, 25νCrg—Cca, (11βC6═O15, 10βC2═O8 in phase), 10βrg
174vw		175	65βCrg—Cca, 10βC—Oca
	164vw	165	78γrg, 12γC═Oca
132vw		138	92γrg
103vw		110	63γrg, 21γCrg—Cca
		61	52γC—Oca, 33γC═Oca, 15γrg,

Intensities: s, strong; m, medium; w, weak; v, very; b, broad; sh, shoulder; ov, overlapped (obtained from the second derivative spectra). The symbols for internal coordinates are as in Tables IV–VI. Only the higher potential energy distribution values are mentioned.

Table VIII. Observed and Scaled Vibrational Fundamentals of N1, N3, O12-^{2}H Deuterated Derivative of Orotic Acid

Observed Wavenumbers		Calculated and Scaled Wavenumbers	
IR $\tilde{\nu}$ (cm^{-1})	Raman $\Delta\tilde{\nu}$ (cm^{-1})	$\tilde{\nu}$ (cm^{-1})	Potential Energy Distribution (%)
3097 m	3097 m	3098	99νC5H14
2360 ov		2359	99νO12D13
2337mb	2331wb	2325	97νN3D9
2317mb	2317 sh	2309	98νN1D7
1734 sh		1726	78νC═Oca
1715 vs	1711 m	1717	66νC2═O8, 8νC6═O15 (in phase)
1632 vs	1638 vs	1678	66νC6═O15, 12νrg, 8νC2═O8(νC═O in opposite phase)
1591 s	1590 w	1594	65νC4C5, 7(other νrg)
1404wb	1415 w	1417	36νN3C4, 14βrg, 23(other νrg)
1334 s	1335 w	1316	26νN1C2, (14βC6═O15, 13βC2═O8 in phase), 13νN3C2, 14(other νrg)
	1293 s	1198	32νN1C6, 26νN1C2, 14βN1D7, 6(other νrg)
1268wb		1213	23νC—Oca, 20βC═Oca, 16βC5H14, 15νCrg—Cca
1162 w	1166 m	1137	29νN3C2, 21νC5C6, 16βN3D9, 9(other νrg)
1068 w	1074 w	1065	44βC5H14, 21(βN1D7, βN3D9), 15(βC2═O8, βC6═O15), 13νrg
964 w	960 m	974	62βrg, 12νC—Oca
910 w	910 w	942	24βOD, 25νC—Oca, 10βN3D9, 12νrg
888 w	881 m	896	29νC—Oca, 22βN3D9, 10νN3C4, 9(other νrg)
857wb		846	61γC5H14, 19γC6═O15, 17γrg
795 m	795vw	831	24νC5C6, 14βN3D9, 12νN3C2, 10νN1C6, 5(other νrg)
774 m		783	(41βN1D7, 16βN3D9 in phase), 11νN1C2, 10νN3C2, 10νN1C6, 5(other νrg)
		774	82γC2═O8, 11γrg
759 sh		752	36γCrg—Cca, 27γC6═O15, 17γC═O15, 10γC2═O8
734 w	734vw	704	35γrg, 29γC6═O15, 17γC5H14, 16γCrg—Cca
692 m	696 m	600	18βC═Oca, 17νrg, 13βOD, 12βrg, 12νC—Oca
621 m	624vw	462	78γN1D7, 12γOD
595mb	599 m	422	85γN3D9, 12γrg
570vw		579	19βC2═O8, 15βC6═O15, 13βC—Oca, 11νrg, 10βrg
542 s	533 w	542	34βrg, 17νrg, 16βC═Oca, 12βOD, 10βC—Oca
505vw	503vw	508	67βrg, 13(βC2═O8, βC6═O15)
456 m	453 w	533	31γrg, 22γN1D7, 17γC—Oca, 16γC═Oca, 13γOD
435wb		419	27βC—Oca, 19βC═Oca, 19νrg, 16(βC6═O15, βC2═O8)
	387 w	393	25βC2═O8, 23βrg, 20βC6═O15, 12νrg, (βC═O in opposite phase)
376 w		363	72γOD, 17γrg
		325	27νrg, 26βCrg—Cca, 11βC6═O15, 11βrg, 7βC2═O8, (βC═O in phase)
171vw		171	65βC4—C10, 12βC—Oca
		163	77γrg, 11γC═Oca
130vw		133	88γrg
103vw		108	62γrg, 23γC4—C10
		61	52γC—Oca, 33γC═Oca, 14γC4—C10

Only the higher potential energy distribution values are mentioned.

cm^{-1} (Table IV). Its isotopic shift to 696 cm^{-1} would be assigned to the calculated wavenumber at 634 cm^{-1} (Table V). The corresponding scaled wavenumbers at 656 (Table VII) and 600 cm^{-1} (Table VIII) would be proposed. The OPD vibrations appear in this region below 900 cm^{-1}. The

amino OPD is calculated at about 600 cm^{-1}. Nevertheless, these vibrations in pyrimidinic bases and their derivatives shift to 890–810 cm^{-1} when the N—H groups are involved in hydrogen bonds.[32] The IR bands at 861 and 831 cm^{-1} that shift to 621 and 595 cm^{-1} upon deuteration (Table VIII, Fig. 4) are accordingly assigned to the amino OPD. The OPDs of the C2═O8, C6═O15, C—Oca, and Crg—Cca bonds contribute to the bands observed in the range of 790–750 cm^{-1}. The in-plane deformation vibrations of the C2═O8, C6═O15, C—Oca, and Crg—Cca bonds appear at lower wavenumbers (607–381 cm^{-1}) than their corresponding OPDs. The in-plane deformation of the Crg—Cca bond makes a dominant contribution to a mode whose fundamental obviously appears at lower wavenumbers: 174 cm^{-1} in IR. The IR bands at 240 and 214 cm^{-1} and the corresponding weak Raman bands at 239 and 216 cm^{-1}, respectively, may be ascribed to complex and delocalized vibrations (crystal lattice vibrations and torsion motions appear in this spectral region) involving the whole molecule.

CONCLUSIONS

The optimized structure for the orotic acid molecule is very close to the structure revealed from X-ray data. The observed differences correspond to hydrogen atoms and the carboxylic group that are probably involved in intermolecular interactions. The scaled *ab initio* DFT Becke3P86/6311G** calculation achieved a reasonable approximation to the observed wavenumbers in most cases (averaged deviations of 3.8 and 3.9% for orotic acid and its isotopomer, respectively). Therefore, this treatment provides a vibrational force field that can be considered useful for the interpretation of the vibrational spectra of orotic acid. An assignment of the IR and Raman spectra of orotic acid and its deuterated derivative was proposed considering the results of this calculation, the isotopic effects, and previous results for related molecules (uracil, thymine, and some derivatives of these molecules). This assignment is the basis for subsequent vibrational studies on the interactions of orotic acid with metal ions and different biomolecules.

The authors are grateful to Dr. V. Almasan of the Institute of Isotopic and Molecular Technology (Cluj-Napoca, Romania) for his help in the synthesis of the orotic acid isotopomer, to Mr. Obregón of the Universidad Nacional de Educación a Distancia (Madrid) for his contribution to the recording of the IR and Raman spectra, and to a reviewer for comments that improved this work.

REFERENCES

1. Bailey, L. E.; Hernanz, A.; Navarro, R.; Theophanides, T. Eur Biophys J 1996, 24, 149–158.
2. Bailey, L. E.; Hernanz, A.; Navarro, R. Nucleos Nucleot 1997, 16, 1041–1044.
3. Bailey, L. E.; Navarro, R.; Hernanz, A. Biospectroscopy 1997, 3, 47–59.
4. Gavira, J. M.; Campos, M.; Diaz, G.; Hernanz, A.; Navarro, R. Vib Spectrosc 1997, 15, 1–16.
5. Gavira, J. M.; de la Fuente, M.; Navarro, R.; Hernanz, A. J Mol Struct 1997, 410–411, 425–429.
6. Hernández, B.; Elass, A.; Navarro, R.; Vergoten, G.; Hernanz, A. J Phys Chem 1998, 102, 4233–4239.
7. Panzeter, P. L.; Ringer, D. P. Biochem J 1993, 293(Part 3), 775–779.
8. Berthelot, M.; Cornu, G.; Daudon, M.; Helbert, M.; Laurence, C. Clin Chem 1987, 33, 2070–2073.
9. Banditt, P. J Chromatogr B 1994, 660, 176–179.
10. MacCann, M. T.; Thompson, M. M.; Gueron, I. C.; Tuchman, M. Clin Chem 1995, 41, 739–743.
11. Sarpotdar, A.; Burr, G. J. J Inorg Nucl Chem 1979, 41, 549–553.
12. Lalart, D.; Dodin, G.; Dubois, J. E. J Chim Phys 1982, 79, 449–453.
13. Bach, I.; Kumberger, O.; Schmidbaur, H. Chem Ber 1990, 123, 2267–2271.
14. Kumberger, O.; Riede, J.; Smidbaur, H. Chem Ber 1991, 124, 2739–2742.
15. Baran, E. J.; Mercader, R. C.; Hueso-Ureña, F.; Moreno-Carretero, M.; Quirós-Olozabal, M.; Salas-Peregrin, J. M. Polyhedron 1996, 15, 1717–1721.
16. Fernandez García, E.; McGregor, J. U. J Dairy Sci 1994, 77, 2934–2939.
17. Akalin, A. S.; Gone, S. Sci Int 1996, 51, 554–556.
18. Ruasmadiedo, P.; Badagancedo, J. C.; Fernandez Garcia, E.; Dellano, D. G.; de los Reyes Gavilán, C. G. J Food Protect 1996, 59, 502–508.
19. Takusawaga, F.; Shimada, A. Bull Chem Soc Jpn 1973, 46, 2011–2019.
20. Mutikainen, I. Ann Acad Sci Fenn Ser A2 1988, 217, 1–39.
21. Letellier, R.; Ghomi, M.; Taillandier, E. Eur Biophys J 1987, 14, 243–252.
22. Person, W. B.; Szczepaniak, K. In Vibrational Spectra and Structure; Durig, J. R., Ed.; Elsevier: Amsterdam, 1993; pp 239–325.
23. Rostkowska, H.; Szczepaniak, K.; Nowak, M. J.; Leszczynski, J.; Kubulat, K.; Person, W. B. J Am Chem Soc 1990, 112, 2147–2160.
24. Gould, I. R.; Hillier, I. H. J Chem Soc Perkin Trans 2 1990, 329–330.

25. Leszczynski, J. J Phys Chem 1992, 96, 1649–1653.
26. Thomas, G. J., Jr.; Tsuboi, M. In Advances in Biophysical Chemistry; Bush, C. A., Ed.; JAI Press: Greenwich, CT, 1993; pp 1–70.
27. Florián, J.; Hrouda, V. Spectrochim Acta 1993, 49A, 921–938.
28. Lagant, P.; Vergoten, G.; Efremov, R.; Peticolas, W. L. Spectrochim Acta 1994, 50A, 961–971.
29. Peticolas, W. L.; Rush, T., III. J Comput Chem 1995, 16, 1261–1270.
30. Rush, T., III; Peticolas, W. L. J Phys Chem 1995, 99, 14647–14658.
31. Aamouche, A.; Berthier, G.; Coulombeau, C.; Flament, J. P.; Ghomi, M.; Henriet, C.; Jobic, H.; Turpin, P. Y. Chem Phys 1996, 204, 353–363.
32. Aamouche, A.; Ghomi, M.; Coulombeau, C.; Jobic, H.; Grajcar, L.; Baron, M. H.; Baumruk, V.; Turpin, P. Y.; Henriet, C.; Berthier, G. J Phys Chem 1996, 100, 5224–5234.
33. Aamouche, A.; Ghomi, M.; Coulombeau, C.; Grajcar, L.; Baron, M. H.; Jobic, H.; Berthier, G. J Phys Chem A 1997, 101, 1808–1817.
34. ASTM Subcommitte on Raman Spectroscopy. Raman Shift Frequency Standards: The McCreery Group Summary (ASTM E 1840); American Society for Testing and Materials: Philadelphia, PA; http://chemistry.ohio-state.edu/~rmccreer/shift.html.
35. Schlegel, H. B.; Gill, P. M. W.; Johnson, B. G.; Wong, M. W.; Foresman, J. B.; Robb, M. A.; Head-Gordon, M.; Replogle, E. S.; Gomperts, R.; Andres, J. L.; Raghavachari, K.; Binkley, J. S.; González, C.; Martin, R. L.; Fox, D. J.; Defrees, D. J.; Baker, J.; Stewart, J. J. P.; Pople, J. A. Gaussian 92/DFT; Gaussian, Inc.: Pittsburgh, PA, 1993; Rev. F.3.
36. Billes, F. D.Sc. Dissertation, Hungarian Academy of Sciences, Budapest, 1990.
37. Susi, H.; Ard, J. S. Spectrochim Acta 1974, 30A, 1843–1853.
38. Ghomi, M.; Letellier, R.; Taillandier, E.; Chinsky, L.; Laigle, A.; Turpin, P. Y. J Raman Spectrosc 1986, 17, 249–255.
39. Letellier, R.; Ghomi, M.; Taillandier, E. Eur Biophys J 1987, 14, 227–241.
40. Slósarek, G.; Zamboni, R. Spectrochim Acta 1991, 47A, 863–874.
41. Woolley, E. M.; Wilton, R. W.; Hepler, L. G. Can J Chem 1970, 48, 3249–3252.
42. M'Boungou, R.; Petit-Ramel, M.; Thomas-David, G. Can J Chem 1987, 65, 1479–1484.
43. Tsuboi, M.; Nishimura, Y.; Hirakawa, A. Y.; Peticolas, W. L. In Biological Applications of Raman Spectroscopy; Spiro, T. G., Ed.; Wiley: New York, 1987; pp 109–179.
44. Viant, M. R.; Fellers, R. S.; McLaughlin, R. P.; Saykally, R. J. J Chem Phys 1995, 103, 9502–9505.
45. Terpinski, J. In Laser Raman Spectrometry; Baranska, H., Labudzinska, A., Terpinski, J., Eds.; Ellis Horwood Ltd.: Chichester, U.K., 1987; pp 121–124.